UNIVERSITÀ DEGLI STUDI FIRENZE
DISEI
DIPARTIMENTO DI SCIENZE PER L'ECONOMIA E L'IMPRESA

Working Papers
Quantitative Methods for Social Sciences

Identifying the number of latent factors of stochastic volatility models

Erindi Allaj, Maria Elvira Mancino, Simona Sanfelici

Working Paper N. 02/2024

DISEI, Università degli Studi di Firenze
Via delle Pandette 9, 50127 Firenze (Italia) www.disei.unifi.it

Identifying the number of latent factors of stochastic volatility models

Erindi Allaj[a,*], Maria Elvira Mancino[b,c], Simona Sanfelici[a,d]

[a]Department of Economics and Management, University of Parma, Italy

[b]Department of Economics and Management, University of Firenze, Italy

[c]INdAM Reseach group GNAMPA, Italy

[d]INdAM Reseach group GNCS, Italy

March 12, 2024

Abstract

We provide a procedure to identify the number of latent factors of stochastic volatility models. The methodology relies on the non-parametric Fourier estimation method introduced by Malliavin and Mancino (2002) and applies to high-frequency data. Based on the Fourier analysis, we first estimate the latent volatility process and then the volatilities and covariances of the processes that are gradually identified, such as volatility of volatility and leverage. The analysis of the eigenvalues spectrum of the Gram matrix can reveal information about the actual number of factors driving the process at hand. We corroborate our analysis by numerical simulations on single and multi factor models. Finally, we apply our methodology to intraday prices from the S&P 500 index futures.

Keywords: non-parametric identification stochastic volatility model, Fourier analysis.

1 Introduction

Accurate specification of asset price dynamics is of crucial importance in financial risk management, pricing and hedging of derivative securities. As is well known in financial mathematics, under the no-arbitrage condition, price processes must be semimartingales. The correct identification of an appropriate semimartingale model can nowadays benefit from the use of high-frequency data in a remarkable way.

A huge amount of work has been done in the last thirty years in order to render the assumptions about the data generating processes of the price series more in line with the empirical evidence. In particular, many models have been proposed to model the volatility coefficient, which is of crucial importance in financial risk management and a key input in any derivative pricing formula. Going beyond the classical Black-Scholes (BS) model, a first class of models assumes a time varying volatility by modelling it as a deterministic function of the underlying asset. Another class of models considers the volatility as an additional latent state variable, which can be correlated with the asset price: models of this kind are called stochastic volatility models, including classical models such as Hull and White (1987), Stein and Stein (1991) and Heston (1993). More recently, models accounting for stochastic leverage and stochastic volatility of volatility have been considered (see Mykland and Wang (2014), Curato (2019), Aït-Sahalia and Jacod (2014), Barndorff-Nielsen and Veraart (2013), Huang et al. (2018), Ruan (2020) and Chen et al. (2022) among others). Discriminating between the class of one factor models and of multi factor stochastic volatility models is important for the pricing of derivative securities.

This paper provides a procedure to identify the number of latent factors of stochastic volatility models (driven by one or more factors). The methodology is non-parametric and does not require knowledge of the functional form of the diffusion term or of the drift. It applies to high-frequency data and is based on the Fourier estimation method introduced by Malliavin and Mancino (2002). In the first step, the latent volatility process is obtained in terms of the Fourier transform of returns. Then the instantaneous volatility can be handled as an observable variable and the procedure can be iterated to estimate the volatilities and covariances of the processes progressively identified, such as volatility of volatility and leverage. The analysis of the eigenvalues spectrum of the Gram matrix can reveal information about the actual number of factors driving the process at hand. Although potentially the method can be iterated to a larger number, we limit our analysis to the case of three factors.

In the literature, several specification tests for diffusion models have been proposed, based

on different estimation methods. Among others, we recall Gouriéroux et al. (1993); Gallant et al. (1997); Chernov et al. (2003). Fermanian and Salanié (2004) have suggested a simulated maximum likelihood estimator obtained by using a kernel density estimator of the simulated data; Altissimo and Mele (2009) have proposed an estimator based on the minimization of weighted distances between non-parametric conditional (or joint) densities estimated from sample data and non-parametric conditional (or joint) densities estimated from data simulated out of the model of interest. All the papers cited above require a complete specification of the drift and diffusion terms and require the time span to go to infinity, keeping the interval between successive observations fixed. However, methods based on low frequency observations may fail to exploit all the informational content of the data. Different specification tests for the functional form of the diffusion term of the process, based on infill asymptotics, require the interval between successive observations to shrink to 0 and are implemented using high frequency observations. Examples are given by Corradi and White (1999); Dette and von Lieres und Wilkau (2003); Dette et al. (2006).

More recently Jacod and Podolskij (2013) developed a method to detect the maximal rank of the volatility process within the framework of infill asymptotics. The main idea is based upon a matrix perturbation method and uses the scaling property of a Brownian motion. Fissler and Podolskij (2017) extended their method to noisy high-frequency data using the pre-averaging approach. Kunimoto and Kurisu (2021) propose a method of detecting the number of latent factors of quadratic co-variation of Itô semimartingales from a set of discrete observations under market microstructure effects, based on the separating information maximum likelihood method. They explore the estimated variance-covariance matrix of latent (efficient) prices of the underlying Itô semimartingales by investigating asymptotically its characteristic roots and vectors. Their procedure is essentially the same as the standard method in statistical multivariate analysis, except the fact that they have latent continuous stochastic processes.

This strand of literature is strictly related to risk management and to other statistical problems, such as testing for market (in)completeness in financial mathematics and testing the local volatility versus stochastic volatility hypothesis. Other econometric measures of systemic risk related to principal component analysis are the connectedness indicators by Billio et al. (2012), based on the principal components analysis and Granger-causality network. These indicators measure the proportion of the market variability explained by the first k principal components and aim to identify increased correlation among the asset returns of financial institutions. In fact,

it is a stylized fact that, in periods of financial distress, the asset correlations, the connectedness of the market and the systemic risk increase. In the same direction goes the market rank indicator (MRI) by Figini et al. (2020) that considers the relation between the largest singular value of a matrix of the return time series and its k smallest singular values. The rationale behind this is that, in times of market excitation and higher correlation, the vectors of the return time series become closer in the linear space containing them. The MRI is related to the notion of condition number, a measure of how close returns are; therefore, the MRI increases in periods of market tensions.

The above mentioned papers try to answer the following question: what is the minimal amount of independent Brownian motions required for modeling a d-dimensional diffusion? Answering this question can give a direct economical interpretation of the financial data at hand. Although based on similar rationale, our aim is more specifically to reveal the latent factors that drive a single price process. Therefore, we are more focused on modeling error and its possible effects on the pricing of derivative securities.

Traditionally, the construction of statistical tests and model calibration procedures requires the use of option data. **However, the outcome of the tests and the quality of the calibration may be rather sensitive to moneyness and maturity of the options. For instance, at the extreme ends of option moneyness the data becomes noticeably less reliable and the estimated parameters can be unstable across different moneyness and maturity classes.** Conversely, the approach followed here simply requires the availability of high frequency observations on the price of the underlying asset and does not require any calibration procedures via option prices. Related papers are, among many others, those of Corradi and Distaso (2007a,b) that provide a testing procedure to discriminate between the classes of one factor (or level dependent) and stochastic volatility models, by comparing two estimators of integrated volatility: one is a kernel estimator (Florens and Zmirou (1993); Bandi and Phillips (2003)), the other is the realized volatility. Under the null hypothesis of a one factor model, both estimators are consistent for the true integrated volatility. Under the alternative hypothesis, the kernel estimator is not consistent, while realized volatility retains the consistency property. Podolskij and Rosenbaum (2012) design new procedures to test the assumption of a local volatility model for the price dynamics against the alternative of a stochastic volatility model. Dette and Podolskij (2008) present tests for the form of the volatility function which are based on stochastic processes of the integrated volatility.

Zu (2015) develops a specification test for stochastic volatility models by comparing the nonparametric kernel deconvolution density estimator of an integrated volatility density with its parametric counterpart. Aït-Sahalia (1996); Zu and Boswijk (2017) propose nonparametric specification tests for stochastic volatility models by comparing the nonparametically estimated return density and distribution functions with their parametric counterparts. Corradi and Swanson (2011) develop tests for comparing the accuracy of predictive densities derived from (possibly misspecified) diffusion models. In particular, they outline a simple simulation-based framework for constructing predictive densities for one-factor and stochastic volatility models. Corradi and Distaso (2006) propose a procedure to test for the correct specification of the functional form of the volatility process within the class of eigenfunction stochastic volatility models. The procedure is based on the comparison of the moments of realized volatility measures such as realized volatility, bipower variation, and modified subsampled realized volatility, with the corresponding ones of integrated volatility implied by the model under the null hypothesis.

Our method is fully non-parametric and takes advantage from the well established ability of the Fourier estimator to estimate iterated co-variation processes from discrete price observations. The analysis of the eigenvalues of the Gram matrix allows to identify the number of latent factors of the data generating process.

The outline of the paper is the following. In Section 2, we present our setting and procedure. In Section 3, we illustrate the Fourier methodology for estimating the number of stochastic factors which are latent in observed financial data. We recall the main existing theoretical results related to the estimators of the entries of the Gram matrix and we provide a consistency result for its eigenvalue estimates. In Section 4, we show numerical evidence of the efficacy of our procedure to discriminate between single and multi factor models. In Section 5, we apply the proposed procedure to intraday prices from the S&P 500 index futures. Finally, Section 6 concludes. The Appendices contain the proofs of some consistency results.

2 The Identification Method

We consider a fairly general class of stochastic volatility models. Let $p(t)$ be the log-asset price observed at time t

$$dp(t) = \alpha(t)dt + \sigma(t)dW_t^1 \tag{1}$$

$$d\sigma^2(t) = \theta(t)dt + \xi(t)\, dW_t^2 \tag{2}$$

$$d\xi^2(t) = \eta(t)dt + v_\xi(t)\, dW_t^3, \tag{3}$$

where W^1, W^2, W^3 are (possibly) correlated Brownian motions on a filtered probability space $(\Omega, (\mathcal{F}_t)_{t\in[0,T]}, P)$. We note that $\sigma^2(t)$ is the (stochastic) volatility process and $\xi^2(t)$ the (stochastic) volatility of volatility process.[1] The processes $\alpha(t)$, $\theta(t)$, $\sigma(t)$, $\eta(t)$, $\xi(t)$, $v_\xi(t)$ satisfy usual regularity conditions in order to guarantee the existence of a unique strong solution (see, e.g. Malliavin (1997)) and to ensure positivity of $\sigma^2(t)$ and $\xi^2(t)$.

The model identification method is based on determining the number of non-zero eigenvalues of the variance-covariance matrix associated to the processes in (1)-(3). More precisely, denote by $\langle\, ,\rangle$ the quadratic (co-)variation operation, and define the following volatilities

$$\langle dp(t)\,,\, dp(t)\rangle/dt := A(t)\,,\ \langle dA(t)\,,\, dA(t)\rangle/dt := B(t)\,,\ \langle dB(t)\,,\, dB(t)\rangle/dt := C(t)\,, \tag{4}$$

and cross-volatilities:

$$\langle dA(t)\,,\, dp(t)\rangle/dt := a(t)\ \ ,\ \langle dB(t)\,,\, dp(t)\rangle/dt := b(t)\,,\ \langle dA(t)\,,\, dB(t)\rangle/dt := c(t)\,. \tag{5}$$

It is immediate to identify that $A(t)$ is the volatility process (i.e., $\sigma^2(t)$ for model (1)), $B(t)$ is the volatility of volatility process (i.e. $\xi^2(t)$ for model (2)), and $C(t)$ is the volatility of the volatility of volatility process (i.e., $v_\xi^2(t)$ for model (3)). On the other side, we recognize $a(t)$ as the leverage process, while $b(t)$ as the covariance process between price and volatility of volatility, and $c(t)$ as the covariance between volatility and volatility of volatility. **The latter processes depend on the assumptions made on the Brownian motions driving the model, e.g., if $d\langle W^1, W^2\rangle_t = \rho(t)dt$ then $a(t) = \rho(t)\sigma(t)\xi(t)$. However, the proposed method is based only on the asset price observations and does not depend on the model governing the various quantities of interest, which are simply required to be Brownian semi-martingales. In the intent of keeping our arguments model-free, we introduce the notations in (4) and (5) to point out the mathematical operations involved in the construction of our identification method, independently of the peculiar shape of the processes in (1)-(3). This will be especially useful for what we are going to do at the end of our paper, namely apply our proposed method to real financial data.**

[1] Along the paper we will use the term volatility process as synonym for variance process.

For every $t \in (0, 2\pi)$, consider the following the 3×3 Gram matrix

$$\Gamma(t) = \begin{pmatrix} A(t) & a(t) & b(t) \\ a(t) & B(t) & c(t) \\ b(t) & c(t) & C(t) \end{pmatrix} \tag{6}$$

and denote by $\lambda_1(t), \lambda_2(t), \lambda_3(t)$ (with $\lambda_1(t) \geqslant \lambda_2(t) \geqslant \lambda_3(t) \geqslant 0$) its eigenvalues. The matrix $\Gamma(t)$ is the variance-covariance matrix for the SDEs system (1)-(2)-(3). This matrix has rank equal to one if W^1, W^2 and W^3 are perfectly correlated, as it is for the level dependent volatility models (like Black-Scholes (BS) or Constant Elasticity of Variance (CEV) model), two in the case of a stochastic volatility model (like Heston model), or three for the stochastic volatility of volatility models.

Our method for identifying the number of latent factors consists of three steps.

(i) First, we estimate in a non-parametric way the entries of the matrix Γ. To this purpose, we exploit the Fourier estimation method developed by Malliavin and Mancino (2002). The Fourier methodology allows us to compute the diffusion coefficients in (1)-(2)-(3), and the covariances, starting from discrete observations of the asset log-price trajectory only. The Fourier transform of the unobservable instantaneous volatility process $\sigma(t),\ t \in [0, T]$, is expressed in terms of the Fourier transform of returns by convolution. Then, the instantaneous volatility can be handled as an observable variable and we can iterate the procedure to compute the volatility of the volatility process as well as the other covariances. We remark that all these processes are recovered pathwise from the observation of a given asset price trajectory.

(ii) Second, we compute the eigenvalues of the estimated Gram matrix and the rescaled processes

$$\gamma(t) := \frac{\lambda_1(t)}{\lambda_1(t) + \lambda_2(t) + \lambda_3(t)} \tag{7}$$

$$\beta(t) := \frac{\lambda_2(t)}{\lambda_1(t) + \lambda_2(t) + \lambda_3(t)} \tag{8}$$

$$\rho(t) := \frac{\lambda_3(t)}{\lambda_1(t) + \lambda_2(t) + \lambda_3(t)}. \tag{9}$$

(iii) Third, the analysis of the rescaled eigenvalues allows us to discriminate between different stochastic volaitlity models. More precisely, if the volatility function $\sigma(t)$ is level dependent, i.e.

σ is only a function of the price $p(t)$ and there are no other factors, then $\beta(t) = \rho(t) = 0$. Conversely, when a stochastic volatility model is considered, the two eigenvalues $\gamma(t)$ and $\beta(t)$ are non-zero quantities. Finally, we obtain three non-zero eigenvalues when a stochastic volatility of volatility model is considered.

We point out again that all the entries of the matrix Γ are pathwise computable by simply applying the Fourier methodology to one time series of asset price observations.

3 Estimation of the matrix entries

In this section we show how to estimate non-parametrically the random functions $A(t)$, $B(t)$, $C(t)$, $a(t)$, $b(t)$, $c(t)$ starting from the asset price observations. The method proposed is based on the Fourier methodology explained in Mancino *et. al.* (2017). The estimation of these processes is admittedly challenging and require the use of high frequency data; however, it is well known that high frequency financial data are contaminated by microstructure noise effects which can destroy the accuracy of the estimation (see, e.g., Aït-Sahalia and Jacod (2014) for an updated discussion). To this aim we exploit the robustness of the Fourier estimator of the volatility to microstructure noise. In fact, as it is documented in Mancino *et. al.* (2017), the Fourier estimator needs no correction in order to be statistically efficient and robust to various type of market frictions: the estimator uses all available data by integration and is able to ignore the high-frequency noise by cutting the highest frequencies. Therefore, when efficiently implemented, the Fourier estimator uses as much as possible of the available price sample path without being excessively biased due to the impact of market frictions. This property will be useful in the empirical exercise of Section 5.

3.1 Estimation of the volatility process A

We assume the general model framework (1-3) holds. By change of the origin of time and rescaling the unit of time, we can always reduce ourselves to the case where the time window $[0, T]$ becomes $[0, 2\pi]$.

The first step consists in the estimation of the Fourier coefficients of $A(t)$ from a discrete unevenly spaced sampling of the log-price process $p(t)$. Consider the sequence of observation times $\mathcal{S}_n := \{0 = t_{0,n} \leqslant t_{1,n} \leqslant \cdots \leqslant t_{k_n,n} = 2\pi\}$ for any $n \geqslant 1$, such that the mesh size of the partition goes to 0, that is $\rho(n) := \max_{0\leqslant h\leqslant k_n-1} |t_{h+1,n} - t_{h,n}| \to 0$ as $n \to \infty$. For any

$j = 1, \ldots, k_n - 1$, denote $\delta_j(p) := p(t_{j+1,n}) - p(t_{j,n})$.

For $|k| \leqslant 2N$, define

$$c_k(A_{n,N}) := \frac{2\pi}{2N+1} \sum_{|s| \leqslant N} c_s(dp_n) c_{k-s}(dp_n), \tag{10}$$

where, for any integer k, $c_k(dp_n)$ is the k-th (discrete) Fourier coefficient of the log-return process, namely

$$c_k(dp_n) = \frac{1}{2\pi} \sum_{j=0}^{k_n-1} e^{-\mathrm{i}kt_{j,n}} \delta_j(p),$$

and the symbol i denotes the imaginary unit, $\mathrm{i} = \sqrt{-1}$. A consistent estimator of the random function $A(t)$ can be obtained by the Fourier-Fejer summation

$$\widehat{A}_{n,N,N_A}(t) := \sum_{|k|<N_A} \left(1 - \frac{|k|}{N_A}\right) c_k(A_{n,N}) e^{\mathrm{i}kt}, \tag{11}$$

where $c_k(A_{n,N})$ is defined in (10).

The central limit theorem for the estimator (11) with a slightly sub-optimal rate and an efficient asymptotic variance is proved in Mancino and Recchioni (2015), while more recently Mancino (Mariotti and Toscano) prove that (11) is an efficient estimator of the spot volatility. The rate of convergence is $n^{-1/4}$, that is the optimal one. More precisely, for any integer $|k| < 2N$ and under the condition $N/n \to 1/2$, the following convergence in probability holds

$$\lim_{n,N\to\infty} c_k(A_{n,N}) = c_k(A),$$

where $c_k(A)$ is the k-th Fourier coefficient of the volatility process $A(t)$. Moreover, under the conditions $N/n \to 1/2$ and $N_A n^{-1/2} \to c_A > 0$, it holds in probability

$$\lim_{n,N,M\to\infty} \sup_{t\in(0,2\pi)} |\widehat{A}_{n,N,N_A}(t) - A(t)| = 0$$

and, for any fixed $t \in (0, 2\pi)$, as $n, N, N_A \to \infty$, the following convergence stable in law holds

$$n^{1/2} N_A^{-1/2} \left(\widehat{A}_{n,N,N_A}(t) - A(t)\right) \to \mathcal{N}\left(0, \frac{4}{3}A^2(t) + \frac{2\pi}{3c_A^2} B(t)\right).$$

3.2 Estimation of the volatility of volatility process B

The Fourier estimation method is particularly suited to build an estimator of the volatility of volatility. In fact, the knowledge of the Fourier coefficients of the latent instantaneous volatility $A(t)$ allows us to handle this process as an observable variable and we can iterate the procedure in order to compute the process $B(t)$.

To compute the instantaneous volatility of volatility $B(t)$ we exploit the approach of Sanfelici *et. al.* (2015); Toscano et al. (2022). Hence, an estimator of the random process $B(t)$ is given by

$$\widehat{B}_{n,N,M,M_B}(t) := \sum_{|k|<M_B} \left(1 - \frac{|k|}{M_B}\right) c_k(B_{n,N,M}) e^{\mathrm{i}kt}, \tag{12}$$

where $c_k(B_{n,N,M})$ is defined as

$$c_k(B_{n,N,M}) := \frac{2\pi}{2M+1} \sum_{|j|\leqslant M} c_j(dA_{n,N}) c_{k-j}(dA_{n,N}) - \mathcal{K} c_k(Q_{n,N,M}), \tag{13}$$

with $c_j(dA_{n,N})$ computed as

$$c_j(dA_{n,N}) := \mathrm{i}\, j\, c_j(A_{n,N}) \tag{14}$$

and[2]

$$c_k(Q_{n,N,M}) := 2\pi \sum_{|j|\leqslant M} c_j(A_{n,N}) c_{k-j}(A_{n,N}).$$

For what concerns the Fourier coefficients (13), the consistency and asymptotic error distribution together with its optimal rate and variance are provided in Toscano et al. (2022), whereas those for the spot quantity (12) in Mancino and Toscano (2023). More precisely, for any integer $|k| < 2N$ and under the conditions $N\rho(n) \to 1/2$, $M\rho(n)^{1/2} \to c_M$, the following convergence in probability holds

$$\lim_{n,N,M\to\infty} c_k(B_{n,N,M}) = c_k(B), \tag{15}$$

where $c_k(B)$ is the k-th Fourier coefficient of the volatility of volatility process $B(t)$. Moreover, under the conditions $N\rho(n) \to 1/2$, $M\rho(n)^{1/2} \to c_M > 0$, $M_B\rho(n)^{1/4} \to c_B > 0$ and $\mathcal{K} = \frac{1}{2}\frac{c_M^2}{2\pi}$, it holds in probability

$$\lim_{n,N,M,M_B\to\infty} \sup_{t\in(0,2\pi)} |\widehat{B}_{n,N,M,M_B}(t) - B(t)| = 0$$

[2] $c_k(Q_{n,N,M})$ is an estimator of the k-th Fourier coefficient of quarticity Mancino and Sanfelici (2012).

and, for any $t \in (0, 2\pi)$, as $n, N, M, M_B \to \infty$, the following convergence stable in law holds

$$\rho(n)^{-1/8}\left(\widehat{B}_{n,N,M,M_B}(t) - B(t)\right) \to \mathcal{N}\left(0, \frac{2\pi}{3}\frac{1}{c_B}C^2(t) + \frac{2}{3}\frac{c_B}{c_M}B^2(t) + \frac{2}{15}c_B\, c_M^3 A^4(t) + \frac{16}{9}c_B\, c_M B(t)A^2(t)\right).$$

Note that the volatility of volatility estimator depends only on the Fourier coefficients of the variance $c_j(A_{n,N})$, which have been estimated formerly. The study of the finite sample properties of this estimator in the presence of microstructure noise can be found in Sanfelici *et. al.* (2015).

3.3 Estimation of the volatility of volatility of volatility process C

As in the previous step, once the Fourier coefficients of the volatility of volatility process $B(t)$ have been estimated, we can estimate the variance function of $B(t)$, denoted by $C(t)$.

An estimator of the Fourier coefficients of $C(t)$ is defined by

$$c_k(C_{n,N,M,L}) := \frac{2\pi}{2L+1}\sum_{|j|\leqslant L} c_j(dB_{n,N,M})c_{k-j}(dB_{n,N,M}), \tag{16}$$

where $c_j(dB_{n,M,N})$ is computed as

$$c_j(dB_{n,M,N}) := \mathrm{i}\, j\, c_j(B_{n,M,N}). \tag{17}$$

Finally, a consistent estimator of the function $C(t)$ can be obtained by the Fourier-Fejer summation given its Fourier coefficients. More precisely

$$\widehat{C}_{n,N,M,L,L_C}(t) := \sum_{|k|<L_C}\left(1 - \frac{|k|}{L_C}\right)c_k(C_{n,N,M,L})\, e^{\mathrm{i}kt},$$

where $c_k(C_{n,N,M,L})$ is defined in (16).

The consistency result for the spot volatility of volatility of volatility estimator under the conditions $N = O(n)$, $M = O(n^{1/2})$, $L = O(n^{1/4})$ and $L_C = O(n^{1/8})$ is proved in Appendix A. The rate and asymptotic error normality is under study.

3.4 Estimation of the leverage process a (covariance price-volatility)

The Fourier estimation method is particularly suited to build an estimator of the leverage, that is the covariance between the stochastic variance process and the asset price process. In fact, the knowledge of the Fourier coefficients of the latent instantaneous volatility $A(t)$ allows us to

handle this process as an observable variable and we can iterate the estimation procedure in order to compute the process $a(t)$ (i.e., the leverage).

To compute the instantaneous covariance $a(t)$ we exploit the multivariate version of Fourier method, see Mancino *et. al.* (2017). Hence, an efficient estimator of the stochastic process $a(t)$ is defined by

$$\widehat{a}_{n,N,M,M_a}(t) := \sum_{|k|<M_a} \left(1 - \frac{|k|}{M_a}\right) c_k(a_{n,N,M}) e^{\mathrm{i}kt},$$

where $c_k(a_{n,N,M})$ is defined in

$$c_k(a_{n,N,M}) := \frac{2\pi}{2M+1} \sum_{|j|\leqslant M} c_j(dp_n) c_{k-j}(dA_{n,N}), \tag{18}$$

and $c_j(dA_{n,N})$ is computed as in (14).

The consistency and suboptimal asymptotic error distribution of the Fourier coefficients are given in Curato and Sanfelici (2015) and Curato (2019), while the Central limit theorem and its optimal rate and variance are given in Mancino and Toscano (2022). The results for the spot quantity can be found in Mancino et al. (2023). More precisely, for any integer $|k| < 2N$ and under the conditions $N\rho(n) \to 1/2$, $M\rho(n)^{1/2} \to c_M$, the following convergence in probability holds

$$\lim_{n,N,M\to\infty} c_k(a_{n,N,M}) = c_k(a),$$

where $c_k(a)$ is the k-th Fourier coefficient of the leverage process $a(t)$. Moreover, under the conditions $N\rho(n) \to 1/2$, $M\rho(n)^{1/2} \to c_M > 0$ and $M_a\rho(n)^{1/4} \to c_a > 0$, it holds in probability

$$\lim_{n,N,M,M_a\to\infty} \sup_{t\in(0,2\pi)} |\widehat{a}_{n,N,M,M_a}(t) - a(t)| = 0$$

and, for any $t \in (0, 2\pi)$, as $n, N, M, M_a \to \infty$, the following convergence stable in law holds[3]

$$\rho(n)^{-1/8} \left(\widehat{a}_{n,N,M,M_a}(t) - a(t)\right) \to \mathcal{N}\left(0, \frac{2\pi}{3}\frac{1}{c_a}\sigma_a^2(t) + \frac{2}{3}\frac{c_a}{c_M}A(t)B(t) + \frac{1}{9}c_M c_a A^3(t)\right).$$

The study of the finite sample properties of the estimator in the presence of microstructure noise can be found in Curato and Sanfelici (2022). Note that the estimator (18) depends only on the Fourier coefficients of the asset log-return $c_j(dp_n)$, that are computed from the real data,

[3] $\sigma_a(t)$ is the volatility of the process $a(t)$.

and on the Fourier coefficients of the variance $c_j(A_{n,N})$, which have been estimated previously.

3.5 Estimation of the process b (covariance price-volatility of volatility)

A consistent estimator of the covariance function between price and volatility of volatility $b(t)$ can be obtained by the Fourier-Fejer summation given its Fourier coefficients (19), more precisely

$$\widehat{b}_{n,N,M,L,L_b}(t) := \sum_{|k|<L_b} \left(1 - \frac{|k|}{L_b}\right) c_k(b_{n,N,M,L}) e^{\mathrm{i}kt},$$

where $c_k(b_{n,N,M})$ is defined in

$$c_k(b_{n,N,M,L}) := \frac{2\pi}{2L+1} \sum_{|j|\leqslant L} c_j(dp_n) c_{k-j}(dB_{n,N,M}), \tag{19}$$

and $c_j(dB_{n,N})$ is computed as

$$c_j(dB_{n,N,M}) := \mathrm{i}\, j\, c_j(B_{n,N,M}). \tag{20}$$

The consistency of the spot price-volatility of volatility covariance estimator under the conditions $N = O(n)$, $M = O(n^{1/2})$, $L = O(n^{1/4})$ and $L_b = O(n^{1/8})$ can be proved with analogous method as for C in Appendix A. The rate and asymptotic error normality is under study.

3.6 Estimation of the process c (covariance volatility-volatility of volatility)

A consistent estimator of the function $c(t)$ can be obtained by the Fourier-Fejer summation given its Fourier coefficients (21), more precisely

$$\widehat{c}_{n,N,M,L,L_c}(t) := \sum_{|k|<L_c} \left(1 - \frac{|k|}{L_c}\right) c_k(c_{n,N,M,L})\, e^{\mathrm{i}kt},$$

where $c_k(c_{n,N,M,L})$ is obtained by

$$c_k(c_{n,N,M,L}) := \frac{2\pi}{2L+1} \sum_{|j|\leqslant L} c_j(dA_{n,N}) c_{k-j}(dB_{n,N,M}), \tag{21}$$

using (14) and (20).

The consistence of the spot volatility-volatility of volatility covariance estimator under the conditions $N = O(n)$, $M = O(n^{1/2})$, $L = O(n^{1/4})$ and $L_c = O(n^{1/8})$ can be proved with analogous method as for C in Appendix A. The rate and asymptotic error normality is under study.

3.7 Uniform consistency of the eigenvalues

Let us denote by $\hat{\Gamma}(t)$ the estimator of the matrix (6)

$$\hat{\Gamma}(t) = \begin{pmatrix} \hat{A}(t) & \hat{a}(t) & \hat{b}(t) \\ \hat{a}(t) & \hat{B}(t) & \hat{c}(t) \\ \hat{b}(t) & \hat{c}(t) & \hat{C}(t) \end{pmatrix} \tag{22}$$

Note that here and in the sequel we omit the subscripts in all the Fourier estimators of the different quantities. Also, let $\hat{\lambda}_1(t)$, $\hat{\lambda}_2(t)$ and $\hat{\lambda}_3(t)$ denote the eigenvalues of the matrix (22).

We are now in the position to state the following consistency result. Assume that $N = O(n)$, $M = O(n^{1/2})$, $L = O(n^{1/4})$, $N_A = O(n^{1/2})$, $M_B = O(n^{1/4})$, $L_C = O(n^{1/8})$, $M_a = O(n^{1/4})$, $L_b = O(n^{1/8})$ and $L_c = O(n^{1/8})$. The following convergence in probability holds

$$\lim_{n\to\infty} \sup_{t\in(0,2\pi)} |\hat{\lambda}_j(t) - \lambda_j(t)| = 0, \tag{23}$$

for $j = 1, 2, 3$.

The proof of Theorem 3.7 in given in Appendix B. A similar proof of this result has been given in Liu and Ngo (2017) for the spot cross volatility matrix of a multidimensional diffusion process.

4 Simulation Study

In this section we validate the theory outlined in the previous section by considering different parametric models. We simulate discrete data from four well-known models, characterized by the presence of one, two or three factors. These models include the classical BS model (Black and Scholes (1973)), the CEV model (Cox and Ross (1976)), the Heston model (Heston (1993)) and the Stochastic Volatility of Volatility (SVV) model (Barndorff-Nielsen and Veraart (2013)).

For each model, firstly, the entries of the matrix (6) are estimated according to the Fourier method presented in Section 3; secondly, the eigenvalues $\hat{\lambda}_1(t)$, $\hat{\lambda}_2(t)$ and $\hat{\lambda}_3(t)$ of the estimated matrix are computed. Finally, the quantities

$$\hat{\gamma}(t) = \frac{\hat{\lambda}_1(t)}{\hat{\lambda}_1(t) + \hat{\lambda}_2(t) + \hat{\lambda}_3(t)} \tag{24}$$

$$\hat{\beta}(t) = \frac{\hat{\lambda}_2(t)}{\hat{\lambda}_1(t) + \hat{\lambda}_2(t) + \hat{\lambda}_3(t)} \tag{25}$$

$$\hat{\rho}(t) = \frac{\hat{\lambda}_3(t)}{\hat{\lambda}_1(t) + \hat{\lambda}_2(t) + \hat{\lambda}_3(t)} \tag{26}$$

are computed and examined.

Notably, in the case of one factor models, both $\beta(t)$ and $\rho(t)$ are null, while for a two factor model both $\gamma(t)$ and $\beta(t)$ are different from zero. Lastly, $\gamma(t)$, $\beta(t)$ and $\rho(t)$ are different from zero in the presence of a three factor model. We expect the estimated quantities to confirm this result.

For each of the four models, we use the Euler-Maruyama discretization scheme to simulate data with a step-size equal to $\frac{2\pi}{21600}$ over the interval $[0, 2\pi]$ (see, e.g., Higham (2001)). The observations are then computed at times $j * \frac{2\pi}{21600}$, where j is an integer satisfying $0 \leqslant j \leqslant 21600$, with a total of 21601 observations.

Based on the indications contained is Section 3, the following choice for the cut-off frequencies is adopted: $N = n/2$, $N_A = n^{1/2}$, $M = N_A/2$, $M_B = (16M)^{1/2}$, $L = M_B/2$, $L_C = (16L)^{1/2}$, $M_a = M_B$, and $L_b = L_c = L_C$. Finally, the Fourier estimates of the Gram matrix are evaluated on $2L_C$ equally spaced points in the interval $(0, 2\pi)$.

Mancino and Sanfelici (2011) prove that the Fourier integrated covariance matrix is positive semi-definite when the Fejér Kernel is used. The result is achieved by assuming the same cutting frequency for each element of the matrix. This cannot be done for the estimation of the Gram matrix (6) because the choice of the various cut-off frequencies in the computation of each entry must fulfill the *Nyquist relation* for the grid sizes in time and frequency domains, as we move from the estimation of the first level quantitity $A(t)$ to the second and third level quantities $B(t)$, $C(t)$, $a(t)$, $b(t)$ and $c(t)$. During our numerical and empirical experiments, in cases where the estimated Gram matrix produces negative eigenvalues, we substitute it with its nearest symmetric positive semidefinite matrix in the Forbenius norm (Higham (1988)).

4.1 Single factor models

In this section we consider two classical single factor models, the BS and the CEV model. These models are characterized by the presence of a single Brownian motion, however they account for different characteristics. In particular, the CEV model is a local volatility model which is well suited to capture the relationship between volatility and asset returns (*leverage effect*).

For the BS model, the log-return is specified as follows

$$dp(t) = \left(\alpha - \frac{1}{2}\sigma^2\right) dt + \sigma dW(t). \tag{27}$$

The drift has no effect on the computation of the elements of the Gram matrix Γ and therefore is set equal to zero for every model considered during our simulations. We take $\sigma = 0.1$ and the initial log-price equal to $\ln(100)$. For the BS model, the matrix (6) degenerates into a matrix having only one non-zero entry, that is $A(t) = \sigma^2$, for any $t \in (0, 2\pi)$. The eigenvalue $\lambda_1(t)$ is then equal to σ^2 and it is the unique eigenvalue different from zero. We expect the same thing to happen to the entries of the estimated matrix $\hat{\Gamma}(t)$. Similarly, $\hat{\gamma}(t)$ should be close to 1, while $\hat{\beta}(t) \approx 0$ and $\hat{\rho}(t) \approx 0$.

In the first two top panels of Figure 1 we plot the log-price $p(t)$, the estimated eigenvalue $\hat{\lambda}_1(t)$, the estimated spot volatility $\hat{A}(t)$ and the constant path of the true volatility. The other two eigenvalues $\hat{\lambda}_2(t)$ and $\hat{\lambda}_3(t)$ are plotted in the remaining panels. According to the theoretical results, the plots are displayed in the interval $(0, 2\pi)$. We remark that the apparent difference between the trajectories of $\hat{\lambda}_1(t)$ and $\hat{A}(t)$ can be justified by the fact that the former is plotted at $2L_C$ points, while the latter on a finer grid with $2N_A$ points. Moreover, the eigenvalues are computed using the Matlab function *eig* and not analytically. The mean and the standard deviation of $\hat{\lambda}_1(t)$ are equal to 0.0103 and 9.5110e-04. Further, $\hat{\lambda}_1(t)$ shows no trend, confirming thus that data result from a BS model with volatility equal to 0.1. The values of the estimated eigenvalue $\hat{\lambda}_2(t)$ have a mean and standard deviation equal to $9.0082e-05$ and $7.4861e-05$, while those of $\hat{\lambda}_3(t)$ equal to $9.2817e-08$ and $1.6388e-07$. As expected, the eigenvalues $\hat{\lambda}_2(t)$ and $\hat{\lambda}_3(t)$ are very close to zero.

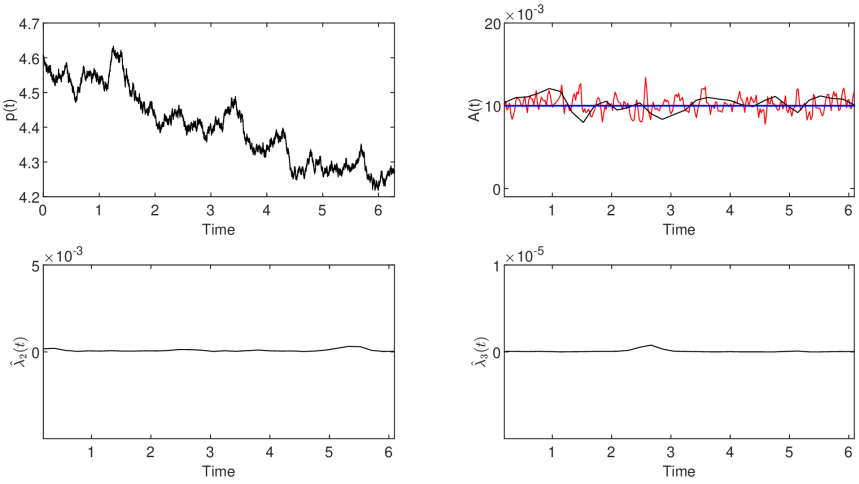

Fig. 1. BS model. Top left panel: The log-price $p(t)$ as a function of time. Top right panel: The Fourier estimate of the spot volatility $A(t)$ is depicted with a solid red line, whereas the estimated eigenvalue $\hat{\lambda}_1(t)$ and the true spot volatility $A(t)$ of the BS model are depicted, respectively, with a solid black and blue line. The bottom two panels plot the estimated eigenvalues $\hat{\lambda}_2(t)$ and $\hat{\lambda}_3(t)$.

Figure 2 represents the behaviour of $\hat{\gamma}(t)$, $\hat{\beta}(t)$ and $\hat{\rho}(t)$. As it can be observed, $\hat{\gamma}(t)$ is almost equal to 1 along the time period and $\hat{\beta}(t)$, $\hat{\rho}(t)$ almost equal to 0, revealing that we are in the presence of a single factor model coherently with the model under study.

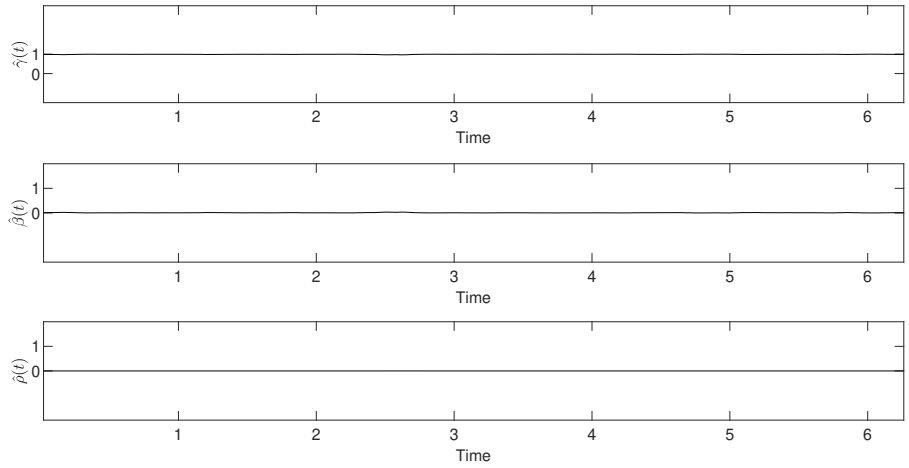

Fig. 2. BS model. The figure shows the values of $\hat{\gamma}(t)$, $\hat{\beta}(t)$ and $\hat{\rho}(t)$.

Indeed, this can also be seen in Table 1 where we report some statistics of $\hat{\gamma}(t)$, $\hat{\beta}(t)$ and $\hat{\rho}(t)$.

Table 1
BS model. Some statistics on $\hat{\gamma}(t)$, $\hat{\beta}(t)$ and $\hat{\rho}(t)$

	Min	Max	Mean	SD
$\hat{\gamma}(t)$	0.9672	1.0000	0.9928	0.0059
$\hat{\beta}(t)$	6.5236e-06	0.0328	0.0072	0.0059
$\hat{\rho}(t)$	0.0000	8.9366e-05	7.8658e-06	1.6236e-05

The table reports the minimum (Min), maximum (Max), mean and the standard deviation (SD) of $\hat{\gamma}(t)$, $\hat{\beta}(t)$ and $\hat{\rho}(t)$.

The second example of one factor model we consider is the CEV model, satisfying the SDE

$$dP(t) = \alpha P(t)dt + \sigma P^{\delta}(t)dW_t, \tag{28}$$

where σ and δ are non-negative constants, and α a constant. A simple application of Itô's formula shows that the log-price $p(t)$ follows the SDE

$$dp(t) = \left(\alpha - \frac{1}{2}\sigma^2\, e^{2p(t)(\delta-1)}\right) dt + \sigma e^{p(t)(\delta-1)} dW_t. \tag{29}$$

We first estimate the entries of the matrix (6) according to the Fourier method presented in Section 3. Secondly, we compute the eigenvalues of the estimated matrix (6). Finally, we obtain the quantities (24 - 26). We expect to obtain a single eigenvalue different from zero, as we are again in the presence of a single factor model, even though the matrix (6) is now a full one.

We highlight the fact that the estimated eigenvalues and the $\hat{\gamma}(t)$, $\hat{\beta}(t)$ and $\hat{\rho}(t)$ paths are obtained in a non-parametric way given only data series of the log-return $p(t)$, therefore showing the feasibility of our method with true empirical data. However, when simulating data out of a parametric model, we can also exploit the knowledge of the parametric model, in order to analytically compute the entries of the matrix (6) for the considered CEV model. In fact, a

simple application of Itô formula yields

$$A(t) := \langle dp(t), dp(t)\rangle/dt = \sigma^2 e^{2p(t)(\delta-1)} \tag{30}$$

$$a(t) := \langle dA(t), dp(t)\rangle/dt = 2\sigma^4(\delta-1)e^{4p(t)(\delta-1)} \tag{31}$$

$$B(t) := \langle dA(t), dA(t)\rangle/dt = 4\sigma^6(\delta-1)^2 e^{6p(t)(\delta-1)} \tag{32}$$

$$b(t) = \langle dB(t), dp(t)\rangle/dt = 24\sigma^8(\delta-1)^3 e^{8p(t)(\delta-1)} \tag{33}$$

$$C(t) := \langle dB(t), dB(t)\rangle/dt = 576\sigma^{14}(\delta-1)^6 e^{14p(t)(\delta-1)} \tag{34}$$

$$c(t) := \langle dA(t), dB(t)\rangle/dt = 48\sigma^{10}(\delta-1)^4 e^{10p(t)(\delta-1)} \tag{35}$$

Filling the matrix $\Gamma(t)$, it is immediate to see that this matrix has rank equal to 1 for every time t, as already anticipated by the fact that CEV has only one Brownian motion, and that the eigenvalues can be computed analytically as follows

$$\lambda_1(t) = A(t) + B(t) + C(t), \qquad \lambda_2(t) = \lambda_3(t) = 0 \tag{36}$$

We recall that the CEV process admits three distinct types of solutions according to the paramenter regimes $\delta < 1/2$, $1/2 \leqslant \delta < 1$ and $\delta > 1$, see Feller (1951). For our simulations, we set $\delta = 0.8$ (i.e. inside of the standard Lipschitz setting/Yamada-Watanabe conditions. Cox and Ross (1976) set $\delta = 0.5$). The CEV model with $\delta < 1$ is characterized by a local volatility which is a decreasing function of the asset price, thus reproducing the so-called leverage effect. The initial log-price is the same as in the BS model.

Figure (3) shows the behaviour of the $\Gamma(t)$ eigenvalues for what concerns the CEV model. It can be noticed that $\hat{\lambda}_1(t)$ and $\lambda_1(t)$ are very close to each other. As in the BS model case, the values of $\hat{\lambda}_2(t)$ and $\hat{\lambda}_3(t)$ are almost equal to zero.

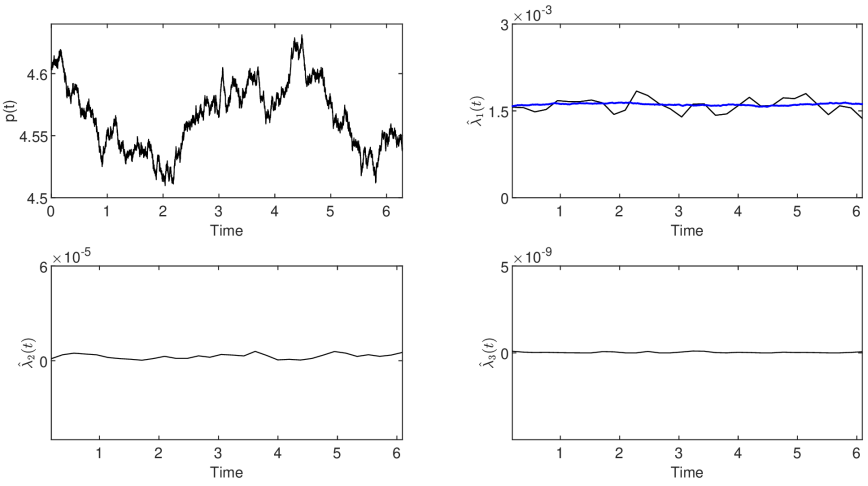

Fig. 3. CEV model. Top left panel: The log-price $p(t)$ as a function of time. Top right panel: The estimated eigenvalue $\hat{\lambda}_1(t)$ is depicted with a solid black line, whereas the true eigenvalue $\lambda_1(t)$ with a solid blue line. The bottom two panels plot the estimated eigenvalues $\hat{\lambda}_2(t)$ and $\hat{\lambda}_3(t)$.

Finally, in Figure 4 we display the values of $\hat{\gamma}(t)$, $\hat{\beta}(t)$ and $\hat{\rho}(t)$, confirming the fact that the values of $\hat{\gamma}(t)$ are almost equal to 1 and those of $\hat{\beta}(t)$ and $\hat{\rho}(t)$ almost equal to 0.

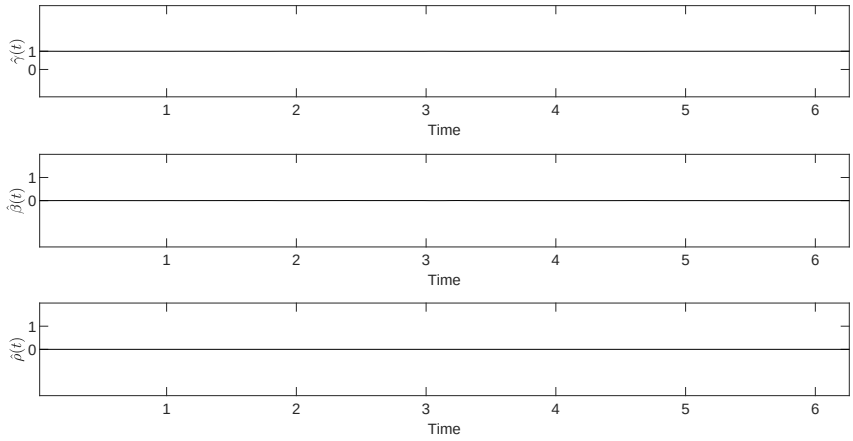

Fig. 4. CEV model. The figure shows the values of $\hat{\gamma}(t)$, $\hat{\beta}(t)$ and $\hat{\rho}(t)$.

4.2 Heston model

Heston (1993) assumes that the volatility process follows a square root model driven by a second

Brownian motion (possibly correlated) with respect to the one driving the asset price. The log-return/variance model has the following form

$$dp(t) = \left(\alpha - \frac{1}{2}\sigma^2(t)\right)dt + \sigma(t)dW_t^1 \tag{37}$$

$$d\sigma^2(t) = \kappa(\theta - \sigma^2(t))dt + \nu\sigma(t)dW_t^2, \tag{38}$$

where W^1, W^2 are correlated Brownian motions, with $\langle dW_t^1, dW_t^2\rangle = \psi dt$. In order to run our simulations, we suppose as in Zhang *et. al.* (2005) that $\kappa = 5$, $\theta = 0.04$, $\nu = 0.5$, and that the correlation coefficient ψ is equal to -0.5. The initial value of the log-price is the same as in the previous models and the initial value of $\sigma^2(t)$ is taken to be equal to 0.1. Observe that the Feller's condition (Feller (1951)) is satisfied.

We begin our analysis verifying the efficiency of the Fourier estimates of the entries of the matrix (6). As for the CEV model, the volatilities (4) and cross-volatilities (5) can be easily obtained in closed-form as follows

$$A(t) := \langle dp(t), dp(t)\rangle/dt = \sigma^2(t), \quad B(t) := \langle dA(t), dA(t)\rangle/dt = \nu^2\sigma^2(t), \tag{39}$$

$$C(t) := \langle dB(t), dB(t)\rangle/dt = \nu^6\sigma^2(t) \quad a(t) := \langle dA(t), dp(t)\rangle/dt = \psi\nu\sigma^2(t), \tag{40}$$

$$b(t) := \langle dB(t), dp(t)\rangle/dt = \psi\nu^3\sigma^2(t), \quad c(t) := \langle dA(t), dB(t)\rangle/dt = \nu^4\sigma^2(t). \tag{41}$$

Figure 5 shows the true and the estimated elements of the matrix $\Gamma(t)$ defined in (6).

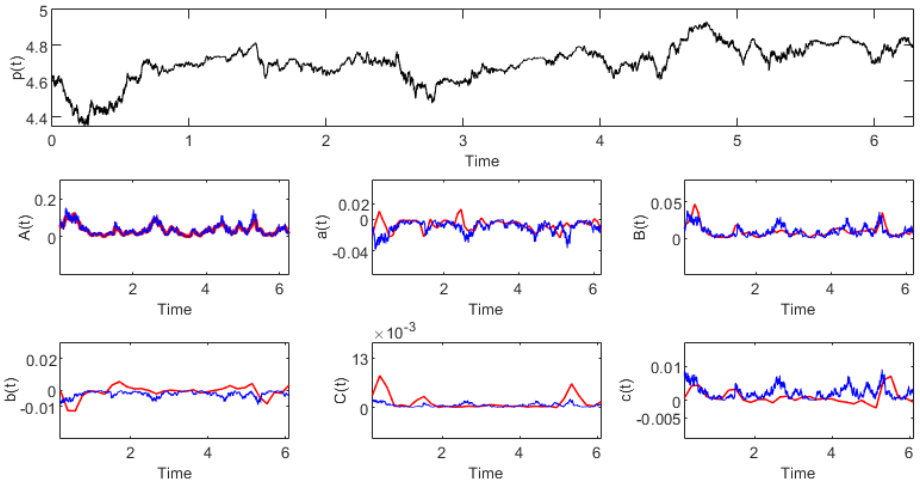

Fig. 5. Heston model. Top panel: The log-price $p(t)$ as a function of time. The middle and bottom panels: The Fourier estimates of the stochastic processes $A(t)$, $a(t)$, $B(t)$, $b(t)$, $C(t)$ and $c(t)$ are depicted with a solid red line, whereas the corresponding true quantities with a solid blue line.

The Fourier estimates are particularly accurate especially in the case of the spot volatility. The estimated leverage process of $a(t)$ is in most of the cases negative capturing the negative correlation between the log-price and the spot volatility.

The Heston model is driven by only two factors. This is confirmed by our proposed methodology. Indeed, as it can be seen from Figure 6, $\hat{\gamma}(t)$ and $\hat{\beta}(t)$ are both clearly different from zero. This means that the second factor starts to be important recommending data are generated from a two factor model. On the other side, the values of $\hat{\rho}(t)$ are small and close to zero.

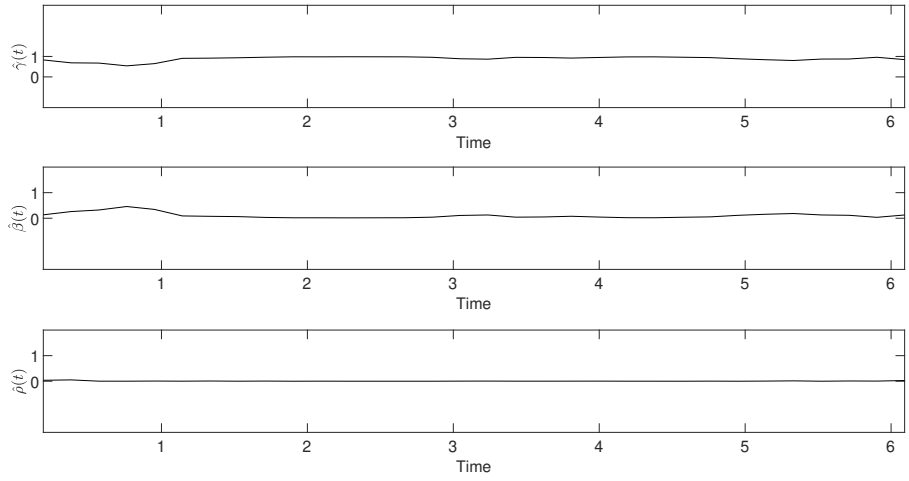

Fig. 6. Heston model. The figure shows the values of $\hat{\gamma}(t), \hat{\beta}(t)$ and $\hat{\rho}(t)$.

The fact that Heston model can be explained by only two factors also emerges from Table 2.

Table 2
Heston model. Some statistics on $\hat{\gamma}(t)$, $\hat{\beta}(t)$ and $\hat{\rho}(t)$

	Min	Max	Mean	SD
$\hat{\gamma}(t)$	0.5403	0.9844	0.8888	0.1108
$\hat{\beta}(t)$	0.0153	0.4586	0.1048	0.1068
$\hat{\rho}(t)$	0.0000	0.0519	0.0064	0.0114

[para,flushleft] The table reports the minimum (Min), maximum (Max), mean and the standard deviation (SD) of $\hat{\gamma}(t)$, $\hat{\beta}(t)$ and $\hat{\rho}(t)$.

We conclude the section by studying the accuracy of the eigenvalue estimators proposed by the Fourier methodology. Computing the characteristic polynomial of the matrix Γ(t) and its analytical eigenvalues, it is found that

$$\lambda_1(t) = \lambda_1\sigma^2(t), \quad \lambda_2(t) = \lambda_2\sigma^2(t), \quad \lambda_3(t) = 0,$$

where

$$\lambda_{1,2} = \frac{(1+\nu^2+\nu^6) \pm \sqrt{(1+\nu^2+\nu^6)^2 - 4(1-\psi^2)(\nu^2+\nu^6)}}{2}.$$

Figure 7 shows the true and the estimated eigenvalues. It can be observed that the values of

the first two eigenvalues (both true and estimated) are different from zero, while $\hat{\lambda}_3(t)$ is almost identically equal to zero as expected.

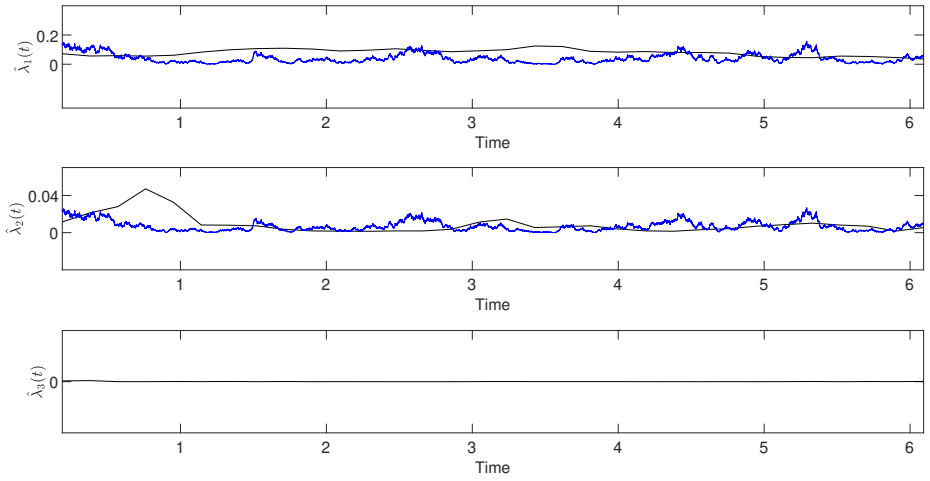

Fig. 7. Heston model. The estimated eigenvalues $\hat{\lambda}_1(t)$, $\hat{\lambda}_2(t)$ and $\hat{\lambda}_3(t)$ are depicted with a solid black line, whereas the true eigenvalues with a solid blue line.

Additionally, the estimated and the true values are relatively close to each other. The slight difference between the true and the estimated eigenvalues can be explained by the fact that if one follows the Nyquist rule, the resolution of the Fourier estimates is lower as one moves from the estimation of $A(t)$ to the other entries of the matrix $\Gamma(t)$ (Mancino and Sanfelici (2020)) and therefore to avoid aliasing effects the matrix eigenvalues can be plotted in a maximum of $2L_C$ points (see also Remark 4). Nevertheless, the approximation still remains good.

4.3 Stochastic Volatility of Volatility model

Barndorff-Nielsen and Veraart (2013) and Kaeck and Alexander (2013) extend existing volatility models to allow for a stochastic specification of the volatility of volatility. As in the Heston model, the log-price in the SVV model is specified as follows

$$dp(t) = \left(\alpha - \frac{\sigma^2(t)}{2}\right) dt + \sigma(t) dW_t^1 \tag{42}$$

We let then the spot volatility be defined by the two factor model (see Sanfelici *et. al.* (2015))

$$d\sigma^2(t) = \kappa(\theta - \sigma^2(t))dt + \xi(t)dW_t^2 \tag{43}$$

$$d\xi^2(t) = \kappa_\xi(\theta_\xi - \xi^2(t))dt + \nu_\xi\xi(t)dW_t^3, \tag{44}$$

where the Brownian motions W^1 and W^2 are correlated with coefficient ψ and W^3 is an independent Brownian motion.

We follow Barletta *et. al.* (2019) and set the parameters of the two factor model as shown in Table 3.

Table 3
SVV model. Parameters of the two factor model (43 - 44)

	κ	θ	κ_ξ	θ_ξ	ν_ξ	ψ
Values	2.26	0.0374	1	0.299	1	0.8

The table reports the values of the parameters κ, θ, κ_ξ, θ_ξ, ν_ξ and ψ.

The initial values of $\sigma^2(t)$ and $\xi^2(t)$ are equal to 0.0324 and 0.299, respectively. The log-price is simulated again with the same parameters of the previous settings. The Feller's condition is not met and therefore the processes $\sigma^2(t)$ and $\xi^2(t)$ might attain negative values. To deal with this problem, we use the Euler-Maruyama discretization with the absorption fix (Korn *et. al* (2010)). De Col et al. (2013) show that the Feller's condition is often violated in practice.

We begin the analysis verifying the efficiency of the Fourier estimator of the entries of the matrix (6). The volatilities and cross-volatilities are easily obtained in closed-form as

$$A(t) = \langle dp(t), dp(t)\rangle/dt = \sigma^2(t), \quad B(t) = \langle dA(t), dA(t)\rangle/dt = \xi^2(t), \tag{45}$$

$$C(t) = \langle dB(t), dB(t)\rangle/dt = \nu_\xi^2\xi^2(t), \quad a(t) = \langle dA(t), dp(t)\rangle/dt = \psi\xi(t)\sigma(t) \tag{46}$$

$$b(t) = \langle dB(t), dp(t)\rangle/dt = 0, \quad c(t) := \langle dA(t), dB(t)\rangle/dt = 0. \tag{47}$$

In particular, the identities show that the leverage effect can be positive or negative depending on the correlation coefficient and that the cross-volatilities between the spot volatility of volatility and the log-price or the spot volatility are zero. The rank of the Gram matrix $\Gamma(t)$, in this case, is full implying the eigenvalues $\lambda_i(t)$, $i = 1, 2, 3$, are different from zero.

The characteristic polynomial is

$$(\nu_\xi^2\xi^2(t)-\lambda)[(\sigma^2(t)-\lambda)(\xi^2(t)-\lambda)-\psi^2\xi(t)^2\sigma(t)^2]=0,$$

thus we have

$$\lambda_1(t)=\nu_\xi^2\xi(t)^2$$

and

$$\lambda_{2,3}(t)=\frac{\xi(t)^2+\sigma^2(t)\pm\sqrt{(\xi^2(t)+\sigma^2(t))^2-4\xi^2(t)\sigma^2(t)(1-\psi^2)}}{2}.$$

Figure 8 shows the accuracy of the Fourier estimates of the matrix $\Gamma(t)$ with respect to the true ones. The results presented in this figure are encouraging for the Fourier estimators as they approximate very well the elements of $\Gamma(t)$. Also look at how the positive correlation between the log-price and spot volatility is captured by the Fourier estimate of the process $a(t)$.

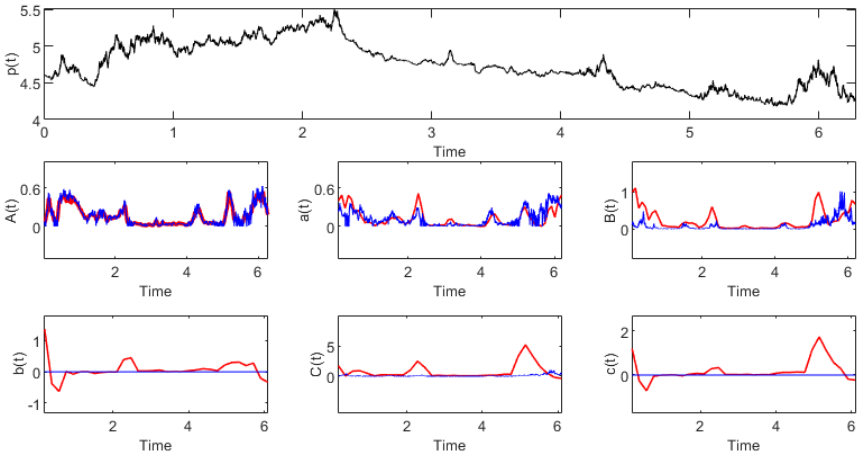

Fig. 8. SVV model. Top panel: The log-price $p(t)$ as a function of time. The middle and bottom panels: The Fourier estimates of the stochastic processes $A(t)$, $a(t)$, $B(t)$, $b(t)$, $C(t)$ and $c(t)$ are depicted with a solid red line, whereas the corresponding true quantities with a solid blue line.

The good performance of the Fourier estimates is also visible from Figure 9. We note that the contribution of the second and third factor increases compared to the previous simulations. More particularly, the third factor starts to become important confirming the fact that the variability of the SVV model is explained by three factors.

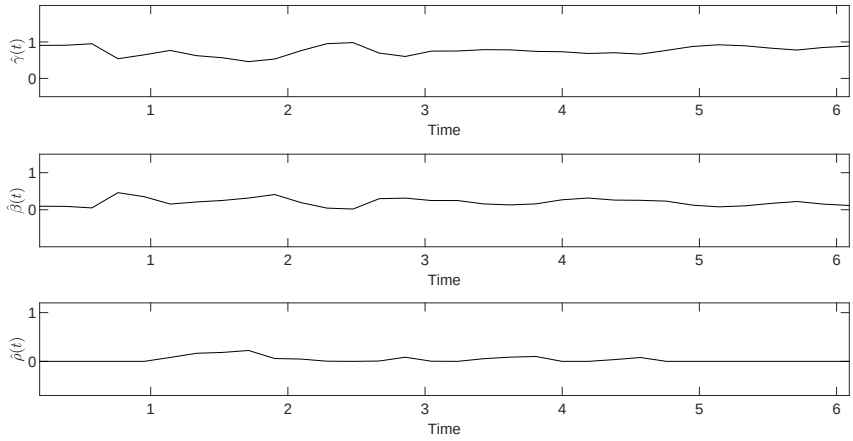

Fig. 9. SVV model. The figure shows the values of $\hat{\gamma}(t)$, $\hat{\beta}(t)$ and $\hat{\rho}(t)$.

The importance of the third factor is also evident from Table 4. Indeed, it can be seen now that the maximum value of $\hat{\rho}(t)$ increases to 0.2230, i.e. one order of magnitude larger than in Table 2.

Table 4
SVV model. Some statistics on $\hat{\gamma}(t)$, $\hat{\beta}(t)$ and $\hat{\rho}(t)$

	Min	Max	Mean	SD
$\hat{\gamma}(t)$	0.4607	0.9809	0.7591	0.1346
$\hat{\beta}(t)$	0.0191	0.4608	0.2030	0.1076
$\hat{\rho}(t)$	0.0000	0.2230	0.0379	0.0602

[para,flushleft] The table reports the minimum (Min), maximum (Max), mean and the standard deviation (SD) of $\hat{\gamma}(t)$, $\hat{\beta}(t)$ and $\hat{\rho}(t)$.

5 Empirical analysis

In order to provide empirical evidence of our results, we apply our proposed non-parametric test to intraday prices from the S&P 500 index futures. This index trades on the Chicago Mercantile Exchange. The tick-by-tick dataset selected for the study covers the period from January 2, 2008 to December 31, 2008 having a total of 251 days.[4] For each day, returns are computed as the difference between two consecutive log-prices. Our dataset includes the collapse of Lehman Brothers, the peak of the global financial crisis of 2007-2008. It would therefore be interesting to see if around this event, a volatility model with more than one factor is more appropriate. Table

[4]We would like to thank Fulvio Corsi for providing data on the S&P 500 index futures.

5 provides some features of these data.

Table 5
Data description

Min	Max	Mean	SD	No. of trades	First trade
739.00	1480.2	1226.55	186.89	557982	09:30

Last trade	Mean trades	Min return	Max return	Mean return	SD return
16:14	5.5165	-0.0866	0.0612	-9.0299e-07	4.7542e-04

The table reports the minimum (Min), maximum (Max), mean and the standard deviation (SD) of the prices and returns of the S&P 500 index futures. In addition, the total number of trades (No. of trades), the lowest and the highest trading time (First and Last trade) and the average number of trades per minute (Mean trades) are reported. The sample covers the period from January 2, 2008 to December 31, 2008 and the number of days is equal to 251.

A necessary step in computing the Fourier estimate of the Gram matrix $\Gamma(t)$ is the determination of the various cutting frequencies involved. As is well known, high-frequency data suffer from microstructure noise. For this reason, for every specific day, a value for the cutting frequency N is derived using the results in Mancino and Sanfelici (2008) with noise moments estimated as in Bandi and Russell (2008). The integrated realized volatility and quarticity estimates required for such derivation are calculated with sparse sampled 10-minute returns, synchronized using the previous tick interpolation method, that is, setting the price to its most recent value. The choice of this sampling frequency is based on the analysis of the volatility signature plot (Andersen *et. al.* (2000)) and the autocorrelation functions (ACFs) shown in Figure 10. From the top two panels (left and middle panels) of this figure it emerges that the microstructure noise is present in our data. Indeed, the left top panel shows that the daily average realized volatility reaches its minimum when computed with raw data and starts then to increase when we lower the sampling frequency. On the other side, from the middle top panel, raw returns have positive autocorrelation at high frequencies. Combining these two facts, we can conclude that the graph shown in the left top panel looks like the volatility signature plot of an illiquid asset (Andersen *et. al.* (2000)). Therefore, the microstructure bias is probably due to inactive trading. This makes sense if we also recall the financial crisis of 2007-2008. Looking also at the other ACFs, it seems natural to assume that returns are noise free when log-prices are recorded at 10-minute intervals.

As pointed out above, for every specific day, the Fourier estimates of the spot volatility are obtained using the previously derived cutting frequency N. The other frequencies are similar to

those in the previous section[5] and are taken equal to $N_A = (8n)^{1/2}$, $M = N_A/2$, $M_B = (16M)^{1/2}$, $L = M_B/2$, $L_C = (8L)^{1/2}$, $M_a = M_B$ and $L_b = L_c = L_C$. In order to avoid cases where the cutting frequencies involved in the computation of the Fourier estimates are too small, we exclude days with less than 1000 trades from our sample leaving us with 240 days.

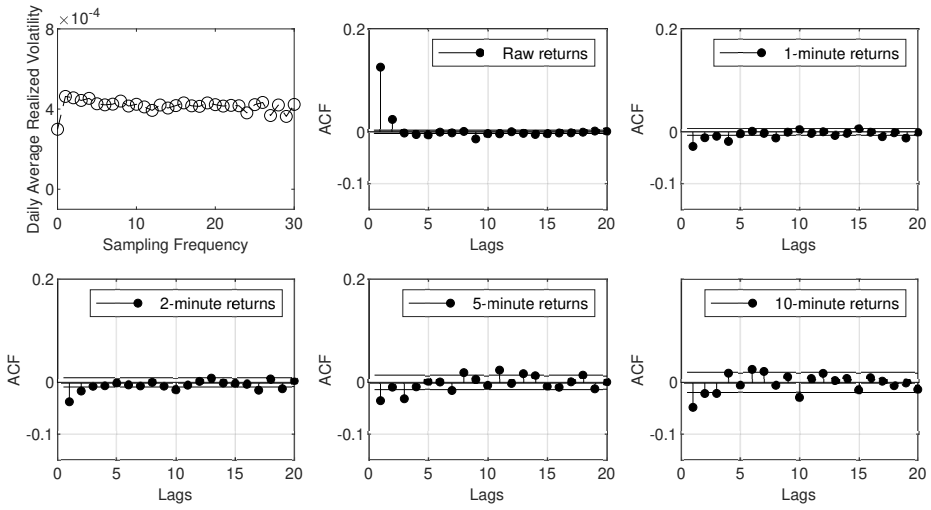

Fig. 10. The top left panel shows the daily average realized volatility as a function of the sampling frequency expressed in minutes. The graph includes also the realized volatility computed with the raw data. The other panels display the autocorrelation functions of raw, 1, 2, 5 and 10-minute returns. The sample covers the period from January 2, 2008 to December 23, 2008 and the number of days is equal to 240.

Equipped with the cutting frequencies, we proceed now to compute the quantities $\hat{\gamma}(t)$, $\hat{\beta}(t)$ and $\hat{\rho}(t)$. For each day of our sample, the estimates are computed at a minimum of 20 and a maximum of 24 points, where as in the previous section we exclude the first and last estimation time. The findings are reported in Table 6 and Figure 11.

[5]Slight differences in the choice of the cut-off frequencies are motivated by the lower average daily number of observations compared to the simulation exercise of Section 4 and the need to maintain a sufficient large number of evaluation points $2L_C$. Nevertheless, we highlight that our results are robust to the sensible choice of the parameters.

Table 6
Some statistics on $\hat{\gamma}(t)$, $\hat{\beta}(t)$, $\hat{\rho}(t)$. $\hat{\lambda}_1(t)$, $\hat{\lambda}_2(t)$ and $\hat{\lambda}_3(t)$

	Min	Max	Mean	SD
$\hat{\gamma}(t)$	0.7171	1.0000	0.9963	0.0124
$\hat{\beta}(t)$	0.0000	0.2819	0.0037	0.0124
$\hat{\rho}(t)$	0.0000	0.0123	1.0412e-05	2.3767e-04
$\hat{\lambda}_1(t)$	1.5020e-06	0.0128	1.1871e-04	4.2712e-04
$\hat{\lambda}_2(t)$	1.8285e-06	0.0012	2.8133e-05	1.0558e-05
$\hat{\lambda}_3(t)$	0.0000	4.3946e-06	3.4117e-09	7.5914e-08

The table reports the minimum (Min), maximum (Max), mean and the standard deviation (SD) of $\hat{\gamma}(t)$, $\hat{\beta}(t)$, $\hat{\rho}(t)$, $\hat{\lambda}_1(t)$, $\hat{\lambda}_2(t)$ and $\hat{\lambda}_3(t)$ for the S&P 500 index futures. The sample covers the period from January 2, 2008 to December 23, 2008 and the number of days is equal to 240.

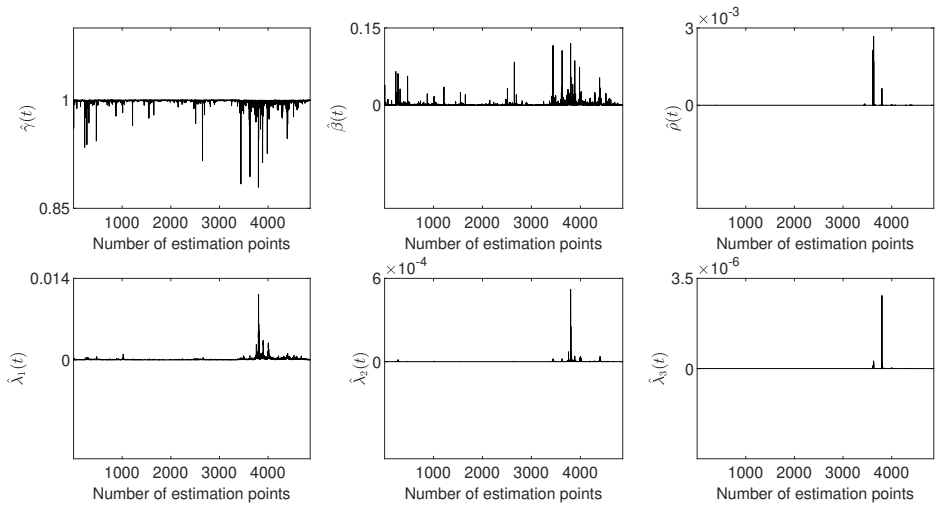

Fig. 11. The top three panels show the values of $\hat{\gamma}(t)$, $\hat{\beta}(t)$ and $\hat{\rho}(t)$. The bottom three panels show the estimated eigenvalues $\hat{\lambda}_1(t)$, $\hat{\lambda}_2(t)$ and $\hat{\lambda}_3(t)$. The sample covers the period from January 2, 2008 to December 23, 2008 and the number of days is equal to 240.

It is interesting to note that the eigenvalues assume relatively low values and that the mean of $\hat{\gamma}(t)$ is approximately equal to one. However, it assumes also a minimum value which is unusual to what we have seen in the previous section for the one factor models. Combining this with the maximum values assumed by $\hat{\beta}(t)$ and $\hat{\rho}(t)$ suggests that there are trading times in which a model with more than one factor can be more adequate. **The results in Table 6 and Figure 11 show that one factor models are adequate to describe the S&P 500 index futures most of the days. This finding is somehow in line with Guyon and Lekeufack (2023),**

where it is empirically shown that the volatility of equity markets is mostly path dependent and do not require considering stochastic volatility models. However, the model proposed in Guyon and Lekeufack (2023) is richer than the one implied by the one factor model considered in the present paper, as we do not consider path dependency in the volatility, but only Brownian semimartingales.

To get a more precise idea of the behaviour of $\hat{\gamma}(t)$, $\hat{\beta}(t)$ and $\hat{\rho}(t)$, we select two specific dates of our sample. The dates are: January 3, 2008 and October 10, 2008. The first date corresponds to the date having the maximum value of $\hat{\gamma}(t)$ and the second to the date having the minimum value of $\hat{\gamma}(t)$. The second date, at the same temporal instant of the minimum value of $\hat{\gamma}(t)$, has a value of $\hat{\beta}(t)$ and $\hat{\rho}(t)$ equal to 0.2819 and 0.0011. **We also tested our dataset for the presence of jumps, which may lead to biased estimates and are usually more proclaimed during crisis periods such as the 2008 financial crisis. Jumps have been identified and measured using the Threshold Bipower Variation method of Corsi et al. (2010), which is based on the joint use of bipower variation and threshold estimation of Mancini (2009). This method provides a powerful test for jump detection, which is employed at the significance level of 99.9%. We refer the reader to Mancino and Sanfelici (2012) for further details on the jump removal procedure. Indeed, the test revealed the occurrence of jumps on many days of the sample that however do not include either January 3 or October 10.**

We plot the corresponding trajectories of $\hat{\gamma}(t)$, $\hat{\beta}(t)$ and $\hat{\rho}(t)$ in Figure 12. Contrary to the top three panels, the bottom panels are much more favourable to a model with more than one factor. Not surprisingly, these panels correspond to the date October 10, 2008 which follows the bankruptcy of Lehman Brothers on September 15, 2008. We would also like to mention here that the maximum value of $\hat{\rho}(t)$, equal to 0.0123, is reached on September 29, 2008 which coincides with the September 29 stock market crash. At the same temporal instant when this value is reached, the values of $\hat{\gamma}(t)$ and $\hat{\beta}(t)$ are equal to 0.8972 and 0.0905. This clearly indicates the presence of more than one latent factor.

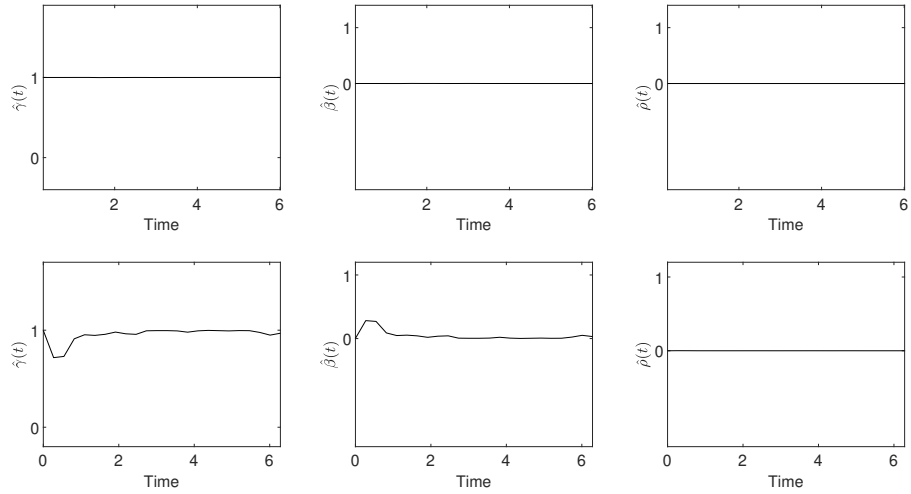

Fig. 12. The top three panels show the values of $\hat{\gamma}(t)$, $\hat{\beta}(t)$ and $\hat{\rho}(t)$ for the day January 3, 2008. The bottom three panels show the values of $\hat{\gamma}(t)$, $\hat{\beta}(t)$ and $\hat{\rho}(t)$ for the day October 10, 2008.

Finally, we show the trending of the log-prices for the days January 3, 2008 and October, 10 2008 in Figure 13. Together with these, the right panels display the scree plots (Cattell (1966)) corresponding to the temporal instants of day January 3, 2008 and October, 10 2008 having, respectively, the maximum values of $\hat{\gamma}(t)$ and $\hat{\beta}(t)$. In the first case (top right panel), the scree plot clearly suggests that a one factor model is correct. On the other hand, the bottom left panel of Figure 13 indicates that there is a higher variability on October, 10 2008. Coherently, the corresponding scree plot in the bottom right panel is more favourable to a two factor model.

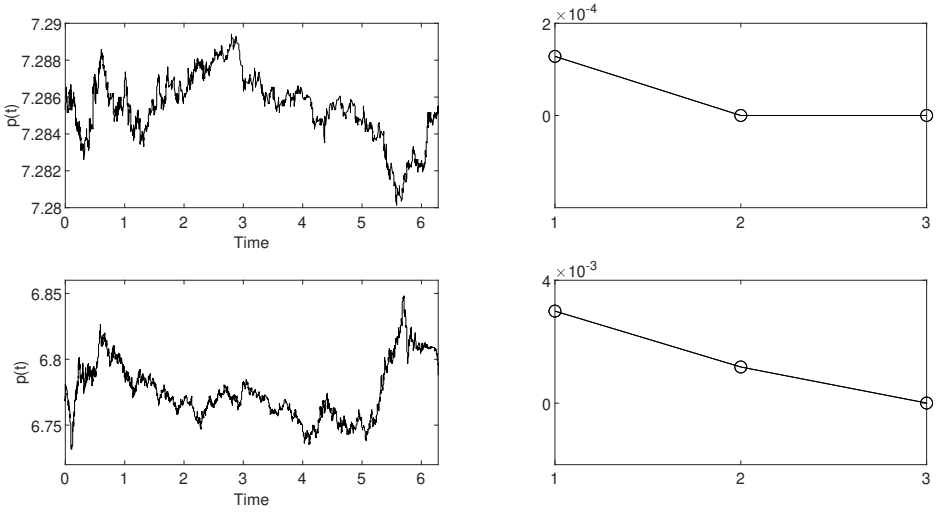

Fig. 13. The left panels show the log-price $p(t)$ for the day January 3, 2008 and October, 10 2008. The right panels show the scree plots corresponding to the temporal instants of day January 3, 2008 and October, 10 2008 having, respectively, the maximum value of $\hat{\gamma}(t)$ and $\hat{\beta}(t)$.

6 Conclusions

The main contribution of the paper is to provide an efficient and easily implementable method to exploit the information contained in the observed asset prices and identify the number of latent factors governing the data generating processes. This issue has many important applications in both risk management and other statistical problems, such as testing for market (in)completeness in financial mathematics and testing the local volatility versus stochastic volatility hypothesis. We propose an efficient non-parametric model to detect the relevant number of factors in the dynamics of the price of a given asset. Our methodology is able to identify factors driving the asset price itself, its volatility and the volatility of the volatility. However, we remark that, potentially, the method can be iterated also to a larger number of factors.

This is made possible by the well established ability of the Fourier estimator to estimate iterated co-variation processes from discrete price observations. Using time series of high-frequency data, the Fourier estimator allows to estimate iterated co-variations filtering out potential microstructure effects. Moreover, while other commonly used estimators, which rely on quadratic-covariation formula, already lose their efficiency when moving to the second iteration, namely the volatility of volatility estimation, and require very long time series and cumbersome choices of the tuning parameters or bias corrections, the Fourier method allows to estimate iterated

co-volatilities even starting from time series of cardinality which are not too big. This can be much relevant for practitioners.

Once the Gram matrix of the estimated processes is composed, the analysis of its eigenvalues allows us to identify the number of latent factors of the data generating process.

The proposed methodology performs very well both numerically and empirically. In particular, our empirical results suggest that it is possible to detect the presence of more factors driving the market in times of crisis and financial turmoil, such as the Lehman Brothers collapse. Overall, we believe our approach can enrich the related literature.

Acknowledgments

This work has been partially supported by the Italian Research Projects of National Relevance (PRIN) P2022AX5TH. We thank the anonymous referee for his/her useful comments.

Ethics declarations

Conflict of interest

The authors declare that they do not have any financial or non-financial conflicts of interest.

A Appendix A

The proof of the consistency for the spot volatility of volatility of volatility estimator is based on the following proposition.

For any integer $|k| < 2N$ and under the conditions $N \sim n$, $M \sim n^{1/2}$, $L \sim n^{1/4}$, the following convergence in probability holds

$$\lim_{n,N,M,L\to\infty} c_k(C_{n,N,M}) = c_k(C),$$

where $c_k(C)$ is the k-th Fourier coefficient of the volatility of volatility of volatility process $C(t)$.

It is enough to prove that the result holds for $k = 0$. The consistency of the other Fourier coefficients estimators follows similarly. In the following we denote by $E[X]$ the expectation for a random variable X. Up to negligible multiplicative constants, we have

$$E[|\frac{2\pi}{2L+1}\sum_{|j|\leqslant L} c_j(dB_{n,N,M})c_{-j}(dB_{n,N,M}) - c_0(C)|^2]$$

$$\leqslant E[|\frac{2\pi}{2L+1}\sum_{|j|\leqslant L} c_j(dB_{n,N})c_{-j}(dB_{n,N,M}) - c_j(dB)c_{-j}(dB)|^2] \tag{48}$$

$$+ E[|\frac{2\pi}{2L+1}\sum_{|j|\leqslant L} c_j(dB)c_{-j}(dB) - c_0(C)|^2]. \tag{49}$$

Remember that the processes involved, follow continuous semimartingale models. First consider (48). It is enough to study the term

$$E[|c_j(dB_{n,N,M})c_{-j}(dB_{n,N,M}) - c_j(dB)c_{-j}(dB)|^2],$$

for any $|j| \leqslant L$. By the Cauchy-Schwartz inequality, this is smaller than

$$E[|c_j(dB_{n,N,M})|^4]^{1/2}E[|c_{-j}(dB_{n,N,M})-c_{-j}(dB)|^4]^{1/2}+E[|c_{-j}(dB)|^4]^{1/2}E[|c_j(dB_{n,N,M})-c_j(dB)|^4]^{1/2}.$$

By the boundedness assumption on the coefficients of the process B_t, the terms $E[|c_{-j}(dB)|^4]$ and $E[|c_j(dB_{n,N,M})|^4]$ are bounded.

We consider now the term

$$E[|c_j(dB_{n,N,M}) - c_j(dB)|^4]^{1/2}.$$

Using the definition, we have

$$E[|c_j(dB_{n,N,M}) - c_j(dB)|^4]^{1/2} = j^2 E[|c_j(B_{n,N,M}) - c_j(B)|^4]^{1/2}. \tag{50}$$

Therefore, the consistency result in (15) and the boundedness of the process B imply that $E[|c_{-j}(B_{n,N,M}) - c_{-j}(B)|^4]^{1/2}$ converges to zero. Further, from the study of the estimator of the process $B(t)$ in Toscano et al. (2022), we derive that it converges with order $o(n^{-1/2})$.

We conclude that (50) goes to zero, observing that that

$$j^2 E[|c_j(B_{n,N,M}) - c_j(B)|^4]^{1/2} = L^2 o(n^{-1/2}) = o(1),$$

for the assumption $L = O(n^{1/4})$.

Now consider (49). From Lemma 3.2 in Malliavin and Mancino (2009) we have

$$E[|\frac{2\pi}{2L+1} \sum_{|j| \leqslant L} c_j(dB) c_{-j}(dB) - c_0(C)|^2] \leqslant K \frac{1}{2L+1} \|B\|_\infty^2,$$

where K is a constant. Letting $L \to \infty$, the consistency follows. □

Based on that, in virtue of the continuity assumption of $C(t)$ (remind that the process $C(t)$ is a Brownian semimartingale), it follows that it holds in probability

$$\lim_{n,N,M,L,L_C \to \infty} \sup_{t \in (0,2\pi)} |\widehat{C}_{n,N,M,L,L_C}(t) - C(t)| = 0.$$

B Appendix B

Let us denote by $\|A\|_2$, $\|A\|_\infty$ the Euclidean and maximum norm of a given $d \times d$ matrix A, respectively. Now, recall that the following inequality holds[6]

$$\|A\|_2 \leqslant \sqrt{d} \|A\|_\infty. \tag{51}$$

The following Lemma provides some bounds on the difference between eigenvalues of the matrix $\hat{\Gamma}(t)$ and $\Gamma(t)$. **(Weyl's Perturbation Theorem)** Let A and $\hat{A}$ be $d \times d$ symmetric

[6]We remind that $\|A\|_2 := \sqrt{\text{maximum eigenvalue of } A^T A}$ and, in particular, for symmetric matrices $\|A\|_2 := \max\{|\lambda_j| : \lambda_j \text{ is an eigenvalue of } A\}$. Moreover, $\|A\|_\infty := \max_{j=1,\dots,d} \sum_{k=1}^d |a_{jk}|$.

matrices and denote by $\lambda_1 \geqslant \lambda_2 \geqslant \ldots \geqslant \lambda_d$ and $\hat{\lambda}_1 \geqslant \hat{\lambda}_2 \geqslant \ldots \geqslant \hat{\lambda}_d$ their eigenvalues. Then

$$\max_{j=1,\ldots,d} |\hat{\lambda}_j - \lambda_j| \leqslant \|\hat{A} - A\|_2.$$

Proof. See Bhatia (2013).

We are now in the position to prove Theorem 3.7.

Proof of Theorem 3.7: The consistency results in the previous sections entail that

$$\lim_{n,M,N,L,N_A,M_B,L_C,M_a,L_b,L_c \to \infty} \sup_{t\in(0,2\pi)} \|\hat{\Gamma}(t) - \Gamma(t)\|_\infty = 0. \tag{52}$$

For any $\bar{t} \in (0, 2\pi)$, applying Lemma B and inequality (51) to each couple of eigenvalues $\hat{\lambda}_j(\bar{t})$ and $\lambda_j(\bar{t})$, for $j = 1, 2, 3$, we get

$$|\hat{\lambda}_j(\bar{t}) - \lambda_j(\bar{t})| \leqslant \sqrt{3}\|\hat{\Gamma}(\bar{t}) - \Gamma(\bar{t})\|_\infty \leqslant \sqrt{3} \sup_{t\in(0,2\pi)} \|\hat{\Gamma}(t) - \Gamma(t)\|_\infty.$$

Taking the supremum over $(0, 2\pi)$ of the left hand side, we get

$$\sup_{t\in(0,2\pi)} |\hat{\lambda}_j(t) - \lambda_j(t)| \leqslant \sqrt{3} \sup_{t\in(0,2\pi)} \|\hat{\Gamma}(t) - \Gamma(t)\|_\infty.$$

Uniform consistency of the j-th estimated eigenvalue as $n, M, N, L, N_A, M_B, L_C, M_a, L_b, L_c \to \infty$ follows from (52). □

References

Aït-Sahalia, (1996). Testing continuous-time models of the spot interest rate. Rev. Financial Studies 9, 385–426.

Aït-Sahalia, Y. and Jacod, J. (2014) High-frequency financial econometrics, Princeton University Press.

Ait-Sahalia, Y. and Kimmel, R. (2005) Maximum likelihood estimation of stochastic volatility models. *Journal of Financial Economics*

Aït-Sahalia, Y. and Xiu, D. (2017) Using principal component analysis to estimate a high dimensional factor model with high-frequency data. *Journal of Econometrics*, 201: 384–399.

Altissimo, F. and Mele, A. (2009), Simulated non-parametric estimation of dynamic model, Review of Economic Studies, 76(2), 413–450.

Andersen, T.G., Bollerslev, T., Diebold, F.X. and Labys, P. (2000). Great realizations. Risk, 13, 105-108.

Bandi, F. and Phillips, (2003)

Bandi, F.M. and Russell, J.R. (2008). Microstructure noise, realized variance, and optimal sampling. The Review of Economic Studies, 75(2), 339-369.

Barndorff-Nielsen, O. and Shephard, N. (2001) Non Gaussian Ornstein-Uhlenbeck-based models and some of their applicationsin financial economics. *Journal of the Royal Statistical Society: Series B*, 63: 167-241.

Barletta, A., Nicolato, E. and Pagliarani, S. (2019) The short-time behavior of VIX-implied volatilities in a multifactor stochastic volatility framework. Mathematical Finance, 29(3), 928-966.

Barndorff-Nielsen, O. and Veraart, A.E.D. (2013) Stochastic volatility of volatility and variance risk premia. *Journal of Financial Econometrics*, 11 (1): 1-46.

Bates D. (1996) Jumps and stochastic volatility: exchange rate processes implicit in Deutschemark options. *Review of Financial Studies*, 9: 69-107.

Bhatia, R. (2013). Matrix analysis (Vol. 169). Springer Science & Business Media.

Billio, M. , Getmansky, M. , Lo, A.W. , Pelizzon, L. (2012), Econometric measures of connectedness and systemic risk in the finance and insurance sectors. *J. Financial Econ.* 104(3), 535–559 .

Black, F. and Scholes, M. (1973) The pricing of options and corporate liabilities. Journal of political economy, 81(3), pp.637-654.

Bollerslev T., Gibson M., and Zhou H. (2004) Dynamic estimation of volatility risk premia and investor risk aversion from option implied and realized volatilities. Mimeo.

Bollerslev, T. and Zhou, H. (2002) Estimating stochastic volatility diffusion using conditional moments of integrated volatility. *Journal of Econometrics*, 109: 33-65.

Cattell, R. B. (1966). The Scree Test For The Number Of Factors. Multivariate Behavioral Research. 1 (2): 245?276.

Chen T-C., Chordia T., Chung S-L. and Lin J-C. (2022) Volatility-of-Volatility Risk in Asset Pricing, *The Review of Asset Pricing Studies*, 12, (1), 289–335.

Chernov, M., Gallant, A. R., Ghysels, E. and Tauchen, G. (2003), Alternative Models for Stock Price Dynamics, Journal of Econometrics, 116, 225–257.

Corradi, V. and Distaso W. (2006) Semi-Parametric Comparison of Stochastic Volatility Models using Realized Measures. *Review of Economic Studies*, 73: 635-667.

Corradi and V. and Distaso W. (2007) Deterministic versus Stochastic Volatility. *Working paper.*

Corradi, V. and Distaso W. (2007) Testing for One Factor Models versus Stochastic Volatility Models in the Presence of Jumps. *Working Paper.*

Corradi, V. and Swanson, N.R., 2011. Predictive density construction and accuracy testing with multiple possibly misspecified diffusion models. J. Econ. 161, 304–324.

Corradi, V. and White, H. (1999), Specification Tests for the Variance of a Diffusion, Journal of Time Series Analysis, 20, 253–270.

Corsi, F., Pirino, D. and Renó, R., Threshold bipower variation and the impact of jumps on volatility forecasting. *J. Econ.*, 159(2), 276–288.

Cox, J.C. and Ross, S.A. (1976) The valuation of options for alternative stochastic processes. *Journal of financial economics*, 3(1-2): 145-166.

Curato, I. (2019) Estimation of the stochastic leverage effect using the Fourier transform method. *Stochastic Processes and their Applications*, 129(9): 3207-3238.

Curato, I. and Sanfelici, S. (2015) Measuring the leverage effect in a high-frequency framework. In: Gregoriou G.N. (ed) *The Handbook of High-Frequency Trading*, Elsevier, Amsterdam, 425–446.

Curato, I. and Sanfelici, S. (2022) Stochastic leverage effect in high-frequency data: a Fourier based analysis. *Econometrics and Statistics*, 23, 53–82.

De Col, A., Gnoatto, A. and Grasselli, M. (2013) Smiles all around: FX joint calibration in a multi-Heston model. Journal of Banking & Finance, 37(10), 3799-3818.

Dette, H. and Podolskij, M. (2008) Testing the parametric form of the volatility in continuous time diffusion models — a stochastic process approach, Journal of Econometrics, 143(1), 56–73.

Dette, H., Podolskij, M. and Vetter, M. (2006) Estimation of Integrated Volatility in Continuous-Time Financial Models with Applications to Goodness-of-Fit Testing, Scandinavian Journal of Statistics, 33(2): 259–278.

Dette, H. and von Lieres und Wilkau, C. (2003), On a Test for a Parametric Form of Volatility in Continuous Time Financial Models, Finance and Stochastics, 7, 363–384.

Duffie D., Singleton K. (1993) Simulated moments estimation of Markov models of asset prices. *Econometrica*, 61: 929-952.

Feller, W. (1951) Two singular diffusion problems. *Annals of mathematics*, 173-182.

Fermanian, J. D. and Salanié, B. (2004), A Nonparametric Simulated Maximum Likelihood Estimation Method, Econometric Theory, 20, 701–734.

S. Figini, M. Maggi, P. Uberti (2020), The market rank indicator to detect financial distress, *Econometrics and Statistics* 14: 63–73.

Fissler, T., and Podolskij, M. (2017). Testing the maximal rank of the volatility process for continuous diffusions observed with noise. *Bernoulli*, 23, 3021-3066.

Florens and Zmirou (1993) FINIRE!

Gallant, A., Hsieh, D. and Tauchen, G. (1997), "Estimation of Stochastic Volatility Models with Diagnostics", Journal of Econometrics, 81, 159-192.

Garcia R., Lewis M., Pastorello S., Renault E. (2006) Estimation of objective and risk neutral distributions based on moments of integrated volatility. Mimeo.

Gouriéroux C., Monfort A. and Renault E. (1993) Indirect inference. *Journal of Applied Econometrics*, 8: S85-S119.

Guyon, J., and Lekeufack, J. (2023). Volatility is (mostly) path-dependent. *Quantitative Finance*, 23(9), 1221–1258.

Harvey A., Ruiz E., Shephard N. (1994) Multivariate stochastic variance models. *Review of Economic Studies*, 61: 247–264.

Heston S. (1993) A closed-form solution for options with stochastic volatility with applications to bond and currency options. *Review of Financial Studies*, 6: 327–343.

Higham, D.J. (2001) An algorithmic introduction to numerical simulation of stochastic differential equations. SIAM review, 43(3), 525-546.

Higham, N.J. (1988) Computing a Nearest Symmetric Positive Semidefinite Matrix, Linear Algebra Appl. 103, 103-118.

Hobson D., Rogers L. (2002) Complete models with stochastic volatility. Mimeo.

Huang D., Schlag C., Shaliastovich I., and Thimme J. (2018) Volatility-of-Volatility Risk. *Published online by Cambridge University Press.*

Hull J. and White A. (1987) The pricing of options on assets with stochastic volatilities. *Journal of Finance*, 42: 281–300.

Jacod, J., and Podolskij, M. (2013). A test for the rank of the volatility process: The random perturbation approach. *The Annals of Statistics*, 41, 2391-2427.

Jacquier E., Polson N., Rossi P. (1994) Bayesian analysis of stochastic volatility models. *Journal of Business and Economic Statistics*, 12: 371–389.

Kaeck, A. and Alexander, C. (2013) Continuous-time VIX dynamics: On the role of stochastic volatility of volatility. *International Review of Financial Analysis*, 28, 46–56.

Korn, R., Korn, E. and Kroisandt, G. (2010) Monte Carlo methods and models in finance and insurance. CRC press.

Kunimoto, N. and Kurisu, D.(2021) Detecting factors of quadratic variation in the presence of market microstructure noise. *Japanese Journal of Statistics and Data Science*, 4:601-641.

Liu, N. and Ngo, H. (2017) Approximation of eigenvalues of spot cross volatility matrix with a view toward principal component analysis, Japan J. Indust. Appl. Math., 34: 747–761.

Malliavin, P. (1997) *Stochastic analysis.* A series of comprehensive studies in mathematics, vol.313. Springer-Verlag, 1997.

Malliavin, P. and Mancino, M.E. (2002). Fourier series method for measurement of multivariate volatilities. *Finance and Stochastics*, 4: 49–61.

Malliavin, P. and Mancino, M.E. (2009). A Fourier transform method for nonparametric estimation of multivariate volatility. *The Annals of Statistics*, 37(4): 1983–2010.

Mancini, C., Non-parametric threshold estimation for models with stochastic diffusion coefficient and jumps. *Scand. J. Stat.*, 36, 270–296.

Mancino, M.E., Oliva, I. and Toscano, G. (2023) Non-parametric estimation of the leverage effect's feedback to price and volatility change. *Working paper*.

Mancino, M.E. and Recchioni, M.C. (2015). Fourier spot volatility estimator: asymptotic normality and efficiency with liquid and illiquid high-frequency data. *PloS one*, 10(9), p.e0139041.

Mancino, M.E., Recchioni, M.C. and Sanfelici, S. (2017) Fourier-Malliavin volatility estimation: Theory and practice. Springer International Publishing.

Mancino, M.E. and Sanfelici, S. (2008). Robustness of Fourier estimator of integrated volatility in the presence of microstructure noise. *Computational Statistics & data analysis*, 52(6), 2966–2989.

Mancino M.E. and Sanfelici S., Covariance estimation and dynamic asset allocation under microstructure effects via Fourier methodology, in *Financial Econometrics Modeling*, G. N. Gregoriou and R. Pascalau Eds., Palgrave-MacMillan, London, UK, 2011, pp. 3–32.

Mancino M.E. and Sanfelici S., Estimation of Quarticity with High Frequency Data, *Quantitative Finance*, 12(4), 607–622

Mancino, M.E. and Sanfelici, S. (2020) Identifying financial instability conditions using high frequency data. *Journal of Economic Interaction and Coordination*, 15(1), 221–242.

Mancino, M.E. and Toscano, G. (2022) Rate-Efficient Asymptotic Normality of the Fourier Estimator of the Leverage Process. *Statistics and Its Interface*, 15 (1), 73–89.

Mancino, M.E. and Toscano, G. (2023) The volatility of volatility risk premium: asymptotic theory and empirical evidence. *Working paper*.

Mancino, M.E., Mariotti, T. and Toscano, G. (2022) Asymptotic Normality for the spot volatility Fourier estimator in the presence of microstructure noise contamination. Working Paper.

Mykland, P.A. and Wang, D. The estimation of leverage effect with high-frequency data. *Journal of the American Statistical Association*, 109(505): 197–215.

Podolskij, M. and Rosenbaum, M. (2012). Testing the local volatility assumption: A statistical approach. Ann. Finance, 8, 31–48.

Ruan X., Volatility-of-volatility and the cross-section of option returns, *Journal of Financial Markets*, 48, 100492.

Sanfelici, S., Curato, I.V. and Mancino, M.E. (2015) High-frequency volatility of volatility estimation free from spot volatility estimates. *Quantitative Finance*, 15(8), 1331–1345.

Stein E., Stein J. (1991) Stock price distributions with stochastic volatility: ana analytic approach. *Review of Financial Studies*, 4: 727–752.

Todorov, V. (2006) Estimation of continuous-time stochastic volatility models with jumps using high frequency data.

[Toscano et al., 2022] Toscano, G., Livieri, G., Mancino, M.E. and Marmi, S. (2022) Volatility of volatility estimation: central limit theorems for the Fourier transform estimator and empirical study of the daily time series stylized facts. Journal of Financial Econometrics, nbac035, https://doi.org/10.1093/jj
nec/nbac035

Yuan, K.H. and Chan, W. (2008) Structural equation modeling with near singular covariance matrices. Computational Statistics & Data Analysis, 52(10), pp.4842-4858.

Y. Zu (2015), Nonparametric specification tests for stochastic volatility models based on volatility density, Journal of Econometrics 187 (2015) 323–344.

Y. Zu and H. P. Boswijk (2017), Consistent nonparametric specification tests for stochastic volatility models based on the return distribution, Journal of Empirical Finance, 41: 53–75.

Zhang, L., Mykland, P.A. and Aït-Sahalia, Y. (2005). A tale of two time scales: Determining integrated volatility with noisy high-frequency data. Journal of the American Statistical Association, 100(472), 1394-1411.